ORIGINAL PAPER

A. Kounov · D. Seward · D. Bernoulli · J.-P. Burg
Z. Ivanov

Thermotectonic evolution of an extensional dome: the Cenozoic Osogovo–Lisets core complex (Kraishte zone, western Bulgaria)

Abstract The Kraishte region of Bulgaria is located at the junction of the Balkanides and Hellenides-Dinarides tectonic belts. Fission-track analysis on both apatites and zircons documents the Cenozoic exhumation of a Precambrian basement bounded by low-angle detachments. Late Eocene–Oligocene extension began prior to 47 Ma and was dominantly in a top-to-the-southwest direction, confirmed by the sense of younging of apatite and zircon ages. This crustal extension controlled the formation of half-graben sedimentary basins on the hanging walls of the detachments. Thermal modelling of these hanging wall units provides evidence for heat transfer across the detachments from a relatively warm rising footwall. From 32 to 29 Ma, pervasive magmatic activity resulted in the emplacement of rhyolitic to dacitic subvolcanic bodies and dykes, along with intrusion of the Osogovo granite. The results give evidence for extension in the southern Balkan older than, and separated from, the Miocene to Quaternary Aegean extension. This might reflect transtension during northeastward extrusion and rotation of continental fragments around the western boundary of Moesia. Eocene–Oligocene extension seems to have been controlled by the distribution of earlier thickening all around the Carpatho-Balkanic orocline, which is reflected by the Cretaceous emplacement of the Morava Nappe in the Kraishte.

A. Kounov · D. Seward · D. Bernoulli · J.-P. Burg (✉)
Geologisches Institut, ETH and Universität Zürich,
Sonneggstrasse, 5, 8092 Zurich, Switzerland
E-mail: jean-pierre.burg@erdw.ethz.ch
Tel.: +41-1-6326027
Fax: +41-1-6321030

Z. Ivanov
Faculty of Geology and Geography,
University Kliment Ochridski, Boulevard Tsar Osvoboditel,
15, 1000 Sofia, Bulgaria

Present address: A. Kounov
Department of Geological Sciences, University of Cape Town,
7700 Rondebosch, Cape Town, South Africa

Introduction

The Alpine Mediterranean mountain system results from subduction and partial obduction of former Mesozoic ocean basins during the collision of Africa, Europe and a number of smaller intervening microplates (Dewey et al. 1973; Boccaletti et al. 1974; Stampfli et al. 1991; Ricou 1994). One of the major remaining questions on this mountain system concerns the Balkan region where north- to east- (eastern Alps, Carpathians) and south- to west-vergent (Dinarides, Hellenides) belts merge and diverge around continental fragments (Burchfiel 1980) previously considered to be ancient microcontinents (Kober 1928) trapped within the Alpine orogenic belt (Fig. 1). Of these fragments, the Rhodope "massif" of southern Bulgaria and northern Greece is now portrayed as a complicated collage of reworked continental and locally oceanic crust and sediments actively involved in several phases of Alpine deformation and metamorphism (Ivanov 1988; Burg et al. 1990; Burg et al. 1996; Liati and Gebauer 1999). The Rhodope also appears to include rock units of the Serbo-Macedonian high-grade metamorphic series (Ricou et al. 1998), so that the tectonic significance of the Serbo-Macedonian crystalline basement requires reassessment in order to understand the orogenic history of this seismically still very active region.

Ongoing research has demonstrated that, perhaps more than collisional deformation, extension-related exhumation of deep continental crust has shaped the Balkan orogenic segments (Bonev et al. 1995; Burg et al. 1996; Kilias et al. 1997; Ricou et al. 1998; Schmid et al. 1998; Krohe and Mposkos 2002). It becomes crucial to determine whether exhumation was a syn- to post-orogenic event or if it is a far-field expression of the supra-subduction extension known farther south, in the
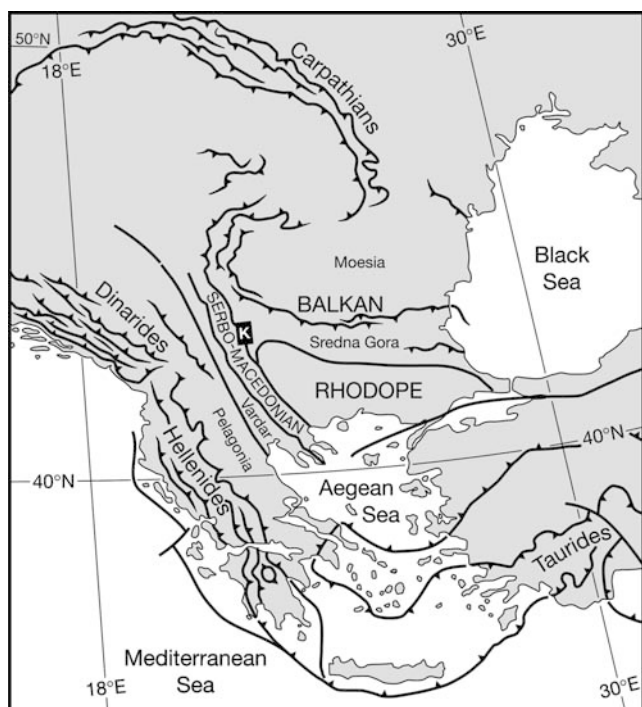
Fig. 1 Location of the study area (*black square* with K for Kraishte) within its Alpine tectonic framework

Aegean realm (Lister et al. 1984; Gautier and Brun 1994; Jolivet et al. 1999). The answer requires time constraints and recognition of the exhumation processes involved.

The relationships between the European and the Rhodope-Macedonian units can be studied in the Kraishte area, in western Bulgaria (Fig. 1). In order to determine the Alpine geological history of this part of the Serbo-Macedonian massif and to clarify its original tectonic position with respect to the surrounding rocks, we applied fission-track analysis on the Vendian-early Cambrian basement and the Oligocene Osogovo intrusions, and to volcanic zircons and apatites of the rhyolites and tuffites interlayered with sediments of the middle Eocene–Oligocene basins. Some Paleozoic, Mesozoic and Paleogene sediments were also analysed in order to complete the regional picture. These new results reveal the particular importance of the Tertiary exhumation history of the Osogovo–Lisets Complex. They constrain the rates of exhumation of the crystalline rocks and provide correlations between basement exhumation, formation of sedimentary basins and volcanic activity. They also document a new example of heat transfer across low-angle extensional normal faults from a relatively warm footwall to the adjacent colder hanging wall.

Geological setting

The Kraishte zone of western Bulgaria is the tectonic area located between the Serbo-Macedonian high-grade metamorphic unit, to the SW, the Rhodope massif to the S and the European margin (late Cretaceous Sredna Gora volcanic arc) to the NE (Fig. 1).

Four major tectono-stratigraphic units are distinguished (Fig. 2):

– The Morava thrust nappe, which has a continental basement and an Ordovician to Devonian sedimentary cover (Spassov 1973; Zagorchev 1984; Zagorchev 1996). It was thrust over the Struma unit during the early Cretaceous (Dimitrov 1931; Bonchev 1936; Zagorchev and Ruseva 1982).
– The Struma unit, which consists of variably deformed continent- and ocean-derived rocks of Vendian—early Cambrian protolith age (Stephanov and Dimitrov 1936; Zagorchev and Ruseva 1982; Haydoutov et al. 1994; Graf 2001; Kounov 2003), unconformably overlain by a Permian to lower Cretaceous sedimentary cover (Zagorchev 1980).
– The Osogovo–Lisets Complex, on which we will concentrate, includes a suite of calc-alkaline plutonic rocks of Vendian—early Cambrian age (Graf 2001; Kounov 2003) and an intrusion of undeformed granite, the Osogovo Granite, dated at 31 ± 2 Ma (Graf 2001).
– The Paleogene basins in which sedimentation was first continental with alluvial deposits (middle Eocene). Late Eocene—early Oligocene turbidites (with intercalated layers of tephra) indicate a change to a deepwater environment of deposition (Moskovski and Shopov 1965; Moskovski 1968, 1969, 1971; Zagorchev et al. 1989). Sedimentation ceased sometime towards the end of the Oligocene. The amount of sediment that was deposited is unknown because some of it has been removed by erosion.

The Osogovo and Lisets Mountains (Fig. 2) form a prominent NW–SE elongated topographic high cored by lower amphibolite-facies (hornblende-garnet-andalusite) metamorphic rocks (Dimitrova 1964). The dome structure was initially interpreted as an old Cadomian (Cambrian) anticline covered by Permian and Triassic sediments (Zagorchev and Ruseva 1982; Zagorchev 1984; Vardev 1987). According to these authors, the supposedly Precambrian or Cambrian amphibolite-facies metamorphic rocks were intruded by Cambrian granitoids and Cambrian or older diorites and granites. The exposure of this basement was attributed to late Alpine extension and the formation of two horsts bounded by steep normal faults in the Lisets and Osogovo Mountains. An alternative interpretation linked the Osogovo–Lisets dome to late Alpine extension accommodated by low-angle detachment faulting and accompanied by retrogression to greenschist facies (Graf 2001).

The Osogovo–Lisets dome is bounded by the Eleshnitsa detachment along its southwestern slope and the Dragovishtitsa detachment on its northeastern side (Fig. 2; Graf 2001). Structural, petrological and geochemical data suggest that the Osogovo–Lisets gneisses

Fig. 2 Geological map of the Kraishte area (SW Bulgaria) modified from Moskovski (1969), Zagorchev and Ruseva (1993) and Zagorchev (1993). *Inset*: geographical location of the map (*black area*)
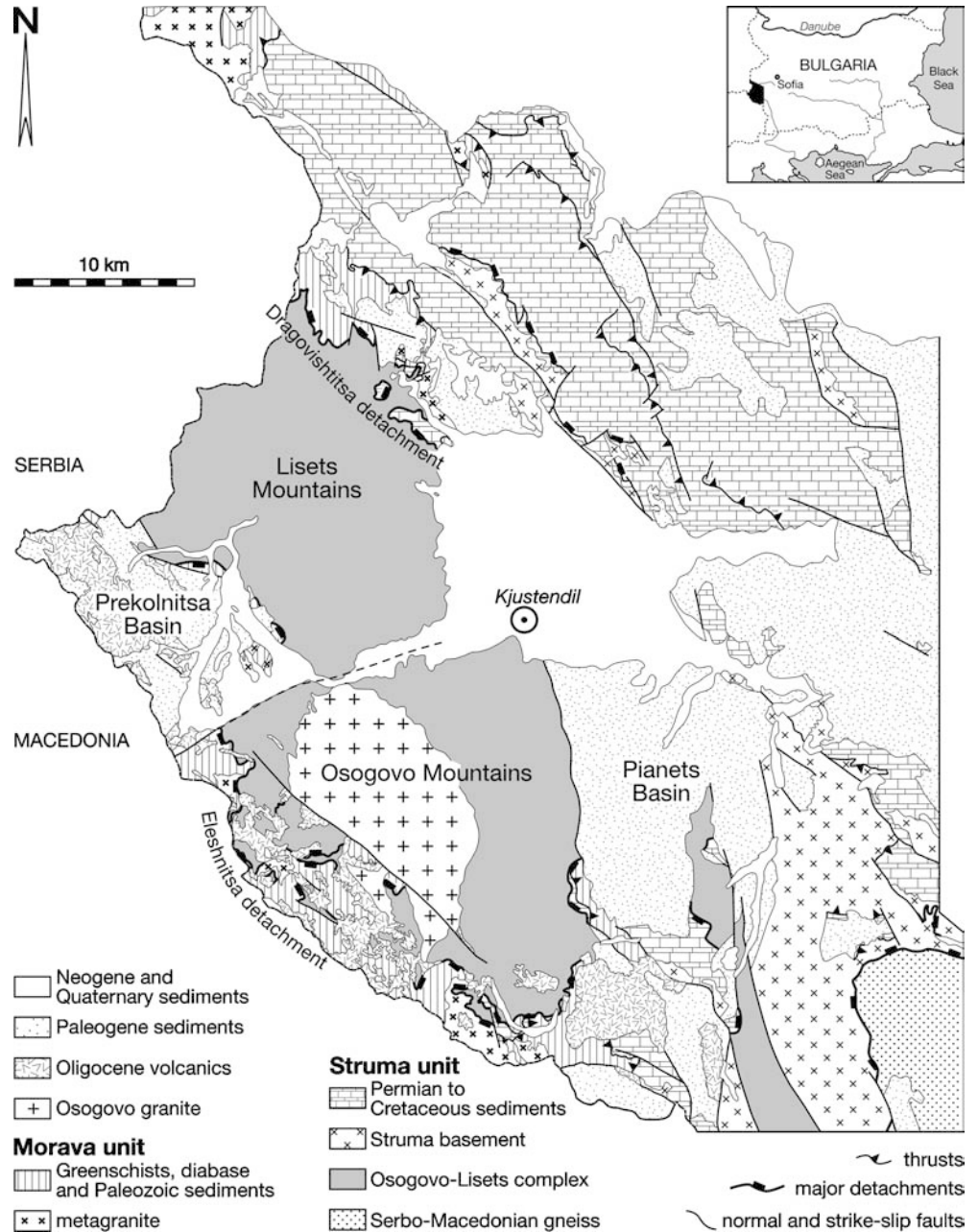
are parts of the Struma basement from which they were separated by the Cenozoic extensional fault system (Graf 2001; Petrov 2001). The Osogovo granite belongs to the W–NW trending Oligocene magmatic belt traced from Turkey through the Balkan Peninsula (Burchfiel et al. 2000).

Cenozoic extension created the sedimentary basins in the hanging wall of the detachments along which structural data indicate generally top-to-the-SW normal faulting. The basin-bounding faults are steep at the surface and cut down into basement; their shape at depth is unknown but they may merge into a low-angle detachment system (Graf 2001). Eocene—Lower Oligocene sediments and their basement are intruded by rhyolitic to dacitic subvolcanic bodies and dykes; the

K/Ar radiometric ages on feldspar phenocrysts and whole rock samples scatter from 30 ± 1 to 32 ± 1 Ma (Harkovska and Pecskay 1997).

Analytical methods and results

The fission-track (FT) analytical procedure is described in the Appendix. Zircon and apatite mineral grains contain the signatures of their cooling histories. Approximate closure temperatures vary according to such factors as chemical composition and rates of cooling. When dealing just with the apparent ages, we use $260 \pm 50°C$ for zircon and $110 \pm 10°C$ for apatite (Green and Duddy 1989; Corrigan 1993; Yamada et al.

1995). Because no chemical compositions were determined for the apatites, the modelled thermal histories were based on the composition of Durango using the Laslett model (Gallagher 1995). The geographical location of the samples and the results are presented in Fig. 3 and Tables 1 to 5.

Morava and Struma units

All samples from the Morava and Struma units yield pre-Cenozoic zircon FT ages (119–69 Ma; Tables 1 and 2). Apatite FT ages from both units can be divided into two groups: (a) 66–56 Ma for samples that have relatively short mean track length (13.18–12.15 μm) and standard deviations of 2.5–1.36 μm; and (b) 40–29 Ma for samples with longer mean track length (14.7–14.29 μm) and standard deviations of 1.54–0.86 μm.

Osogovo–Lisets Complex

Eleven samples from the Osogovo–Lisets Complex were analysed. The majority of the samples cluster between 47 and 39 Ma for zircon and between 46 and 38 Ma for apatite (Fig. 3, Table 3). Exceptions are apatite ages from samples *AK218*, *K1067a*, and *AK45*, which are between 30 and 27 Ma (Fig. 3, Table 3).

In general, samples from the Osogovo–Lisets Complex have long mean track lengths (14.65–13.72 μm) and yield similar zircon and apatite ages (Table 3). Compilation of the modelled time-temperature (T–t) paths (Gallagher 1995) reveals two groups with different thermal histories (Fig. 4). One group underwent fast cooling through both the zircon and apatite closure temperatures from 47 to 38 Ma, while the other cooled more slowly below 110°C after 30 Ma.

Fig. 3 Geological map of the Kraishte area (Fig. 2) with location and FT ages of the analysed samples. Lines AB and CD are the sections in Fig. 8
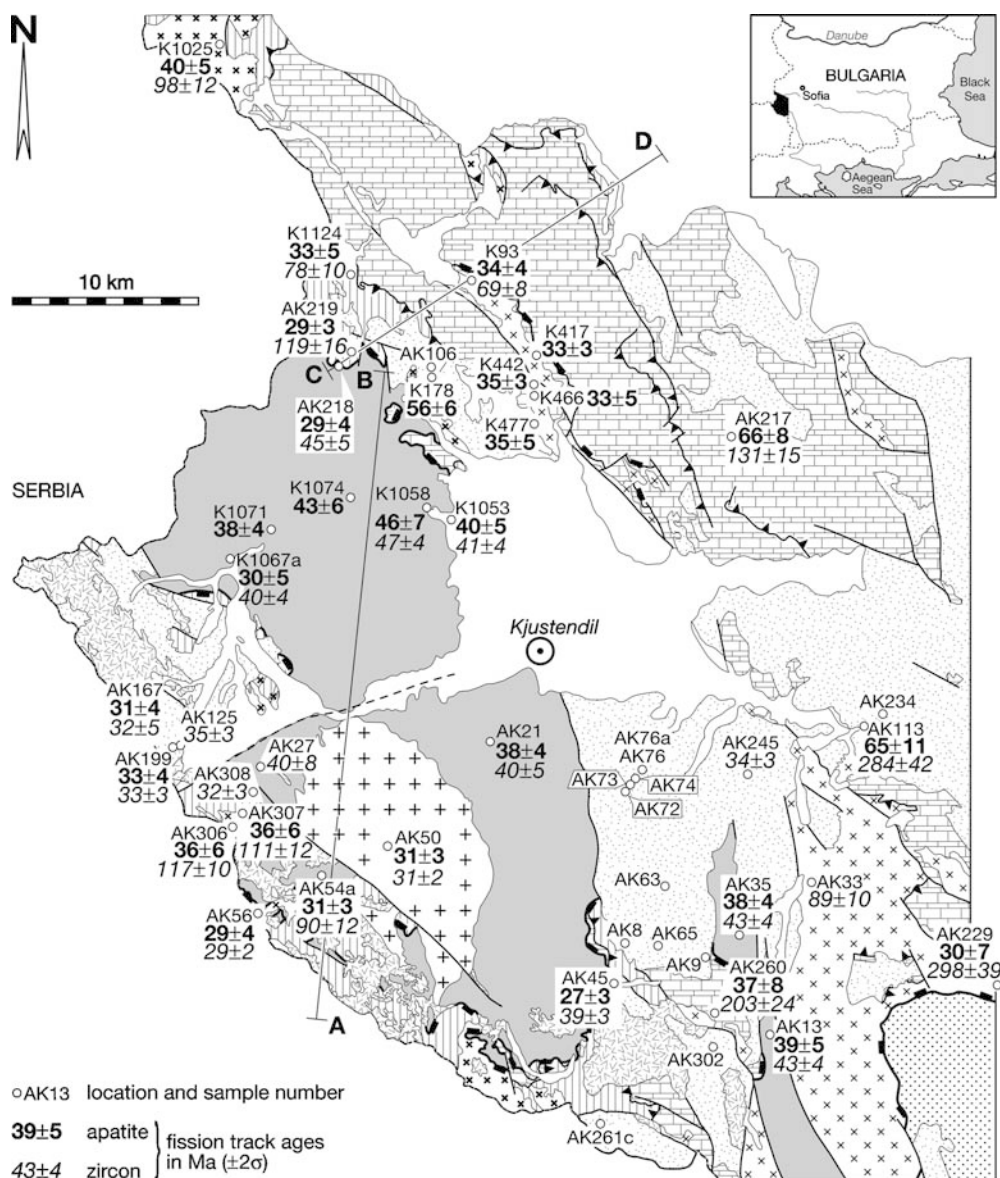
Table 1 Fission-track analysis

Sample no.	Grid references	Altitude (m)	Lithology	Mineral	No. of grains	ρd (10^6 cm^-2)	ρs (10^6 cm^-2)	ρi (10^6 cm^-2)	P(χ²) (%)	Variation (%)	U conc. (ppm)	Central age (±2σ) (Ma)	MTL (±1σ) (μm)	SD (N) (μm)
Morava unit														
K178	N42.40793/E022.62106	780	Granite	A	20	1.177 (6507)	0.6546 (524)	2.563 (2052)	98	<1	27	**55.7±5.6**	12.74±0.27	2.5 (87)
K1025	N42.57330/E022.48878	1,060	Granite	A	20	1.426 (6,507)	0.2716 (270)	1.799 (1788)	54	3	19	**40.0±5.4**	14.32±0.21	0.91 (18)
				Z	20	0.4087 (2,747)	17.34 (1,607)	4.727 (438)	54	7	451	*98.4±11.8*		
K1124	N42.46169/E022.56913	825	Diabase	A	20	1.015 (11,478)	0.2783 (225)	1.577 (1,275)	72	2	19	**33.3±4.8**	14.29±0.12	0.86 (52)
				Z	16	0.4030 (2,747)	8.759 (1,101)	2.983 (375)	95	0	289	*77.7±9.8*		
AK219	N42.41828/E022.57276	640	Sandstone	A	18	1.003 (3,262)	0.9207 (407)	5.861 (2,591.2)	96	0	73	**29.2±3.2**	14.37±0.13	0.91 (52)
				Z	18	0.2899 (2,093)	13.64 (1,675)	2.179 (267.6)	99	0	301	*118.7±16.4*		
AK306	N42.20429/E022.50826	1,851	Granite	A	20	1.175 (4,578)	0.3069 (178)	1.883 (1,092.4)	89	0	20	**35.5±5.8**	14.46±0.19	1.4 (53)
				Z	20	0.3970 (2,761)	10.86 (3,431)	2.418 (764)	90	0	238	*116.6±10.4*		
AK307	N42.21171/E022.52372	1,698	Granite	A	21	1.213 (4,578)	0.35 (170)	2.165 (1,051.5)	90	0	70	**36.4±6.2**	14.3±0.17	1.34 (63)
				Z	18	0.3883 (2,761)	14.51 (2,110)	3.322 (483)	98	0	334	*111.0±12.0*		

P(χ²) is the probability of obtaining χ² values for ν degrees of freedom where ν = number of crystals−1
All ages are central ages (Galbraith 1981). λD = 1.55125x10^−10
A geometry factor of 0.5 was used
Zeta = 372 ± 13 for CN5/apatite, and 132 ± 3 for CN1/zircon
Irradiations were performed at the ANSTO facility, Lucas Heights, Australia
All numbers in brackets are numbers of measurements
ρd, ρs and ρi represent the standard, sample spontaneous and induced track densities, respectively
A apatite, Z zircon, MTL mean track length

Paleogene sediments

By applying the FT technique to apatites, the timing and the temperature of burial of the sediments as well as the final inversion of each basin can often be assessed.

Five volcanic ashes were dated both by FT and U/Pb SHRIMP on zircons to better constrain the timing of sedimentation in the basins (Table 4). The zircon FT ages range between 35 and 32 Ma (AK72, AK125, AK167, AK199, AK245; Table 4) in statistical agreement with the U/Pb SHRIMP ages obtained from samples AK199(33.46 ± 0.22 Ma) and AK245(33.07 ± 0.28 Ma) (Fig. 5; Kounov 2003).

Three sandstone samples from the stratigraphically deepest section of the Pianets basin (AK8, AK9, AK65; Fig. 6) each contain only one apatite population, with ages ranging between 48 and 40 Ma and with mean-track lengths from 13 to 12 μm. These ages are very close to the estimated age of deposition (middle Eocene = Bartonian; Kounov 2003). Thermal modelling of these samples (Fig. 7) reveals that there has been post-depositional heating to about 90°C. A similar thermal history may be suggested for the granite clast from a breccia at the base of the small basin N of Kjustendil (AK106, Fig. 3). This sample yields an apatite age of 65 ± 9 Ma with a mean track length of 12.58 ± 0.2 μm and a bimodal length distribution (Fig. 7).

Upwards in the section of the Pianets basin, the apparent apatite ages, except for the uppermost sample (AK234), are older than the depositional age. Attempts to statistically split these into sub populations failed in many cases. This was specifically a problem in some ash layers (e.g. AK73 and AK76, Fig. 6) where the mean ages are at least 10 million years older than the age of sedimentation and hence it was suspected that older detrital populations might be a contaminant. In sample AK76A, the sandstone layer resting on tuff AK76 (Fig. 6), two populations were present in the 50 dated apatite grains (Table 4). The AFT age of the youngest population is 36 ± 1 Ma, which corresponds to the age of the lowermost ash layer AK72 (35.1 ± 3.6) from the same section, as well as to that of a pyroclastic flow AK125 (35.0 ± 3.0) from the Prekolnitsa basin (W of Kjustendil, Figs. 2 and 3). The second population has an age of 49 ± 5 Ma, an age which is slightly older than the oldest age from the Osogovo–Lisets Complex.

All clastic horizons, as well as some of the pyroclastics, contain zircons older than the age of sedimentation; however, there is a general younging trend in these detrital ages upwards in the section (Fig. 6).

Magmatic rocks

Three samples from Cenozoic granites and dykes were dated (Table 5).

The FT analysis of the Osogovo granite yields identical apatite and zircon ages of 31 ± 3 Ma and 31 ± 2 Ma

Table 2 Fission-track analysis

Sample no.	Grid references	Altitude (m)	Lithology	Mineral	No. of grains	ρd (10⁶ cm⁻²)	ρs (10⁶ cm⁻²)	ρi (10⁶ cm⁻²)	$P(\chi^2)$ (%)	Variation (%)	U conc. (ppm)	Central age (±2σ) (Ma)	MTL (±1σ) (μm)	Standard deviation (N) (μm)
Struma unit: basement														
K93	N42.46148/E022.65220	922	Orthogneiss	A	20	1.185 (11,017)	0.4275 (410)	2.83 (2,714)	61	1	30	**34.0±3.6**	14.07±0.19	1.03 (31)
				Z	14	0.4201 (2,747)	15.09 (1,253)	6.022 (500)	99	0	559	*69.1±7.8*		
K417	N42.41866/E022.68948	630	Orthogneiss	A	20	1.147 (11,017)	0.1027 (1,085)	6.88 (7,265)	<1	13	75	**32.5±3.0**		
K466	N42.40207/E022.68874	822	Gabro	A	20	1.121 (11,017)	0.1394 (205)	8.987 (1,322)	74	<1	10	**33.1±5.0**		
AK33	N42.17604/E022.57912	550	Granite	Z	26	0.4011(2,721)	11.40 (2,050)	3.365 (605.3)	12	15	327	*89±10.4*		
AK54a	N42.17468/E022.56020	2,030	Metadiorite	A	15	1.314 (8,505)	0.7754 (534)	6.111 (4,209)	100	0	58	**31.0±3.0**	14.68±0.11	0.99 (81)
				Z	22	0.4400 (2,722)	9.157 (1,049)	2.933 (336)	98	0	260	*90.0±11.8*		
AK113	N42.24827/E022.89954	445	Granite	A	22	0.9981 (5,493)	0.3348 (189)	0.9530 (537.9)	99	0	12	**65.0±11.2**	12.15±0.32	2.25 (49)
				Z	20	0.3687 (2,093)	22.37 (2,658)	1.873 (222.5)	97	0	198	*284.3±41.6*		
AK229	N42.12651/E022.99138	480	Diorite	A	8	0.7650 (3,262)	0.4825 (94)	2.253 (439)	91	0	37	**30.4±7.0**	14.06±0.14	1.40 (105)
				Z	20	0.3868 (2,093)	20.60 (3,579)	1.727 (300)	63	6	174	*297.8±39.0*		
Struma unit: sedimentary cover														
K442	N42.40703/E022.68504	760	Sandstone	A	20	1.134 (11,017)	0.7023 (828)	4.385 (5,170)	30	9	48	**34.5±3.0**	13.99±0.14	1.25 (81)
K477	N42.38740/E022.69192	765	Sandstone	A	20	1.159 (11,017)	0.5639 (331)	3.561 (2,090)	29	14	38	**34.8±4.8**	13.18±0.15	1.36 (83)
AK217	N42.37055/E022.81052	1,005	Sandstone	A	20	1.055 (5,493)	0.611(412)	1.800 (1,213.7)	92	0	2	**66.3±7.8**		
				Z	27	0.3503 (2,093)	20.84 (3,357)	3.610 (581.4)	14	14	402	*131±15.0*		
AK260	N42.11145/E022.80584	951	Sandstone	A	13	1.408 (4,783)	0.2774 (88)	1.976 (626.9)	99	0	18	**36.7±8.4**	14.45±0.19	1.54 (64)
				Z	21	0.4185 (2,761)	27.20 (2,825)	3.636 (377.6)	95	0	339	*203.4±23.6*		

$P(\chi^2)$ is the probability of obtaining χ^2 values for v degrees of freedom where v = number of crystals−1

All ages are central ages (Galbraith 1981). $\lambda D = 1.55125 \times 10^{-10}$

A geometry factor of 0.5 was used

Zeta = 372±13 for CN5/apatite, and 132±3 for CN1/zircon

Irradiations were performed at the ANSTO facility, Lucas Heights, Australia

All numbers in brackets are numbers of measurements

ρd, ρs and ρi represent the standard, sample spontaneous and induced track densities, respectively

A apatite, *Z* zircon, *MTL* mean track length

Table 3 Fission-track analysis

Sample no.	Grid references	Altitude (m)	Lithology	Mineral	No. of grains	ρd (10⁶ cm⁻²)	ρs (10⁶ cm⁻²)	ρi (10⁶ cm⁻²)	P(χ²) (%)	Variation (%)	U conc. (ppm)	Central age (±2σ) (Ma)	MTL (±1σ) (μm)	Standard deviation (N) (μm)
Osogovo–Lisets Complex														
K1053	N42.33860/	595	Orthogneiss	A	28	1.481(6,507)	0.2104 (294)	1.441 (2,013)	76	4	12	**40.1 ± 5.2**	14.13 ± 0.21	1.02 (25)
	E022.64512			Z	21	0.4830 (2,747)	5.245 (1,248)	4.089 (973)	84	0	330	***40.8 ± 3.8***		
K1058	N42.34947/	615	Orthogneiss	A	21	1.068 (11,478)	0.1641 (209)	0.7018 (894)	100	0	8	**46.3 ± 7.2**	14.20 ± 0.28	1.27 (20)
	E022.62037			Z	26	0.4945 (2,747)	6.755 (2,098)	4.643 (1,442)	78	<1	366	***47.3 ± 3.8***		
K1067a	N42.32230/	800	Orthogneiss	A	21	1.095 (11,478)	0.1868 (190)	1.261 (1,283)	37	4	14	**30.2 ± 4.8**	14.62 ± 0.24	1.01(18)
	E022.50214			Z	15	0.4716 (2,747)	7.538 (1,217)	5.853 (945)	93	0	484	***40.0 ± 3.8***		
K1071	N42.33649/	770	Orthogneiss	A	26	1.121 (11,478)	0.4326 (652)	2.357 (3,553)	22	7	26	**38.4 ± 3.6**	14.40 ± 0.09	0.84 (101)
	E022.52591													
K1074	N42.35117/	710	Orthogneiss	A	22	1.232 (6,507)	0.3772 (479)	2.031 (2,579)	2	19	21	**42.8 ± 5.6**		
	E022.57124													
AK13	N42.09224/	650	Metagranite	A	23	1.595 (4,618)	0.5264 (328)	4.018 (2,504)	99	0	32	**38.8 ± 4.6**	14.34 ± 0.13	1.08 (71)
	E02284344			Z	20	0.4835 (2,805)	5.697 (1,406)	4.243 (1,047)	95	0	342	***42.7 ± 3.8***		
AK21	N42.24069/	1,150	Orthogneiss	A	24	1.229 (8,643)	0.3299 (551)	1.958 (3,271)	96	0	20	**38.4 ± 3.6**	14.44 ± 0.10	0.93 (81)
	N022.66421			Z	19	0.3856 (2,721)	1.604 (714)	1.0089 (448.7)	90	0	102	***40.4 ± 5.2***		
AK27	N42.23070/	1,050	Orthogneiss	Z	6	0.4608 (2,805)	7.718 (270)	5.803 (203)	96	0	491	***40.3 ± 7.6***		
	E022.51599													
AK35	N42.14760/	602	Metagranite	A	25	1.332 (4,240)	0.3748 (363)	2.461 (2,383.2)	77	<1	23	**37.7 ± 4.4**	14.65 ± 0.14	0.6 (20)
	E022.82332			Z	19	0.4244 (2,722)	4.450 (1,247)	2.866 (803)	84	0	263	***43.4 ± 4.2***		
AK45	N42.12663/	695	Metagranite	A	23	1.421 (8,643)	0.3062 (299)	3.015 (2,944.4)	100	0	27	**26.8 ± 3.4**	13.72 ± 0.26	1.73 (46)
	E022.74389			Z	20	0.4178 (2,644)	3.999 (2,354)	5.654 (1,665)	81	<1	373	***38.9 ± 3.0***		
AK218	N42.41653/	680	Orthogneiss	A	19	1.170 (5,493)	0.4237 (322)	3.156 (2,398.4)	80	0	34	**29.2 ± 3.6**	14.46 ± 0.12	0.73 (40)
	E022.56809			Z	11	0.3081 (2,093)	26.11 (1,237)	11.86 (561.9)	87	0	1,540	***44.6 ± 5.0***		

$P(\chi^2)$ is the probability of obtaining χ^2 values for v degrees of freedom where v = number of crystals−1

All ages are central ages (Galbraith 1981). $\lambda D = 1.55125 \times 10^{-10}$

A geometry factor of 0.5 was used

Zeta = 372 ± 13 for CN5/apatite, and 132 ± 3 for CN1/zircon

Irradiations were performed at the ANSTO facility, Lucas Heights, Australia

All numbers in brackets are numbers of measurements

ρd, ρs and ρi represent the standard, sample spontaneous and induced track densities, respectively

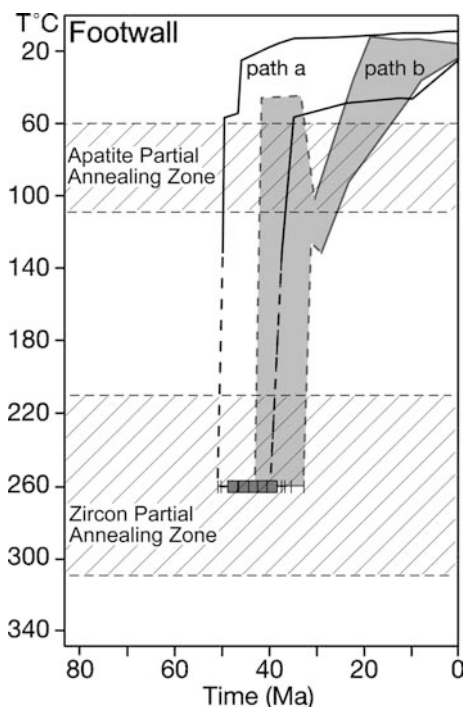*A* apatite, *Z* zircon, *MTL* mean track length

Fig. 4 Modelled T–t paths for footwall samples (crystalline rocks of the Osogovo–Lisets Complex) of the detachment system. For details of modelling see the Appendix. Group "a" shows fast cooling from 47 to 38 Ma. Group "b" underwent relatively slower cooling after 30 Ma. The apatite partial annealing zone is within the temperature limits assigned by Laslett et al. (1987). The modelled T–t paths are extended into the zircon partial annealing zone (Yamada et al. 1995) where *grey squares* represent the zircon FT ages of the modelled samples

(*AK50*; Fig. 3), respectively. The mean track length in apatite is 14.53 ± 0.10 μm. These ages are concordant with the U/Pb zircon single crystal ages of Graf (2001). Rhyolitic dykes yield zircon FT ages of 32 ± 3 and 29 ± 2 Ma (*AK308* and *AK56*; Fig. 3) and an apatite age of 29 ± 4 Ma (*AK56*) with a mean track length of 15.07 ± 0.1 μm.

Interpretation

This discussion refers to the structural frame summarised above, whereby the Osogovo–Lisets Dome represents the footwall of a Cenozoic extension system characterised by the major Eleshnitsa detachment and the Morava and Struma units forming, along with the sedimentary basins, the hanging wall.

Thermal history of the footwall

Compilation of the modelled T–t paths from the Osogovo–Lisets Complex reveals two groups with different thermal histories (Fig. 4). Group "a" had very rapid cooling from 260 to 60°C between 47 and 38 Ma. This rapid cooling is also confirmed by the almost identical

ages of the zircons and apatites. Samples from group "b" yielded similar zircon ages. We suggest that they also followed path "a" until they reached 60°C and afterwards they underwent a heating event prior to 30 Ma before cooling to the surface from that time on. Rhyolitic dykes and small igneous bodies ubiquitously intruded the detachments at 31 Ma and most likely caused local heating to temperatures >110°C (*K1067a, AK45, AK218*), resetting any previous apatite ages (Fig. 4, path "b"). Effects of such intrusions are by chance of sampling. Thus the FT ages of group "b" are considered to indicate such local thermal perturbations on the overall general cooling pattern.

The cooling path "a" traces rapid exhumation of the Osogovo–Lisets Complex, which reflects a major tectonic event. Extension-related exhumation along the Eleshnitsa detachment is the most likely interpretation, and began before 47 Ma. Progressive southwestward unroofing and cooling along this detachment is observed through the decreasing zircon and apatite FT ages (Fig. 8). A maximum extension rate may be derived, using the width of the exhumed rocks along which the younging trend is measured. This yields an average of 2 mm/year over 7 million year. We emphasise that this value might be overestimated by as much as 40% (Ehlers et al. 2001), yet is a reasonable figure in terms of tectonic processes.

Thermal history of the hanging wall

Morava and Struma units

The two groups of apatite FT ages from the Morava and Struma units are interpreted as follows:

– The modelled T–t paths of the 66–56 Ma samples (path "c", Fig. 9) take into account that the sample sites were just underneath the Paleogene sediments and that clasts from the Morava and Struma units are present in these sediments. Thus the Morava and Struma units are assumed to have been at or very close to the surface during the Paleogene. The thermal histories reveal a period of heating to a maximum of 100°C between 48 and 35 Ma before cooling again to the surface today.
– The second group "d", reveals a period of cooling through the apatite partial annealing zone over the last 40 million year.

The timing of this heating phase in the hanging wall is coincident with the extension phase that exhumed the Osogovo–Lisets Complex. We suggest that this heating event is most likely due to heat advecting from the rising hot footwall rocks.

Basins

The syn-sedimentary volcanic rocks have zircon ages between 35 and 32 Ma (Fig. 6). Therefore, the oldest

Table 4 Fission-track analysis

Sample no.	Grid references	Altitude (m)	Lithology	Mineral	No. of grains	ρd (10^6 cm^{-2})	ρs (10^6 cm^{-2})	ρi (10^6 cm^{-2})	P(χ^2) (%)	Variation (%)	U conc. (ppm)	Central age ($\pm 2\sigma$) Ma	MTL ($\pm 1\sigma$)μm	Standard deviation (N) μm
Cenozoic terrigeneous sediments														
AK8	N42.14432/E022.75207	1,015	Sandstone	A	32	1.306 (4,240)	0.5221 (962)	3.171 (5,842)	20	10	30	**39.9±3.4**	13.26±0.2	1.6 (49)
				Z	29	0.4948 (2,805)	6.252 (7,412)	2.290 (2,715)	0	32	181	**88.2±11.6**		
AK9	N42.14067/E022.80550	710	Breccia	A	28	1.435 (8,505)	0.3603 (216)	2.000 (1,199)	77	1	17	**48.0±7.2**	11.70±0.49	2.58 (28)
				Z	22	0.4890 (2,651)	28.06 (3,452)	3.935 (484)	99	0	314	**226.2±23.6**		
AK63	N42.17429/E022.77501	685	Sandstone	A	43	1.649 (6,294)	0.3243 (707)	2.151 (4,689.3)	99	0	16	**46.1±3.8**	14.85±0.11	0.87 (63)
				Z	41	0.4065 (2,644)	11.85 (3,666)	3.178 (982.8)	0	39	305	**96.1±14.4**		
AK65	N42.14149E022.77235	895	Sandstone	A	34	1.535 (6,294)	0.4725 (875)	3.258 (6,034.2)	71	1	27	**41.3±3.2**	13.26±0.2	1.7 (65)
				Z	31	0.4462 (2,644)	16.68 (4,662)	5.213 (1,656.7)	0	20	456	**93.7±9.6**		
AK76A	N42.22664/E022.76065	630	Sandstone	A	50	1.541(8,643)	0.6808 (1,376)	3.416 (6,905.7)	0	30	28	**56.7±6.2**	13.64±0.18	1.45 (65)
				Z	36	0.4665 (2,805)	12.17 (6,844)	4.416 (2,483)	0	32	369	**85.0±10.6**		
AK106	N42.42128/E022.62260	900	Breccia	A	20	1.119 (4,578)	0.4873 (300)	1.563 (962)	97	0	18	**64.6±8.8**	12.58±0.22	2.25 (108)
				Z	18	0.3754 (2,761)	9.524 (2,662)	1.685 (471)	84	<1	175	**138.5±14.8**		
AK234	N42.25183/E022.90947	470	Sandstone	A	23	1.171 (3,787)	0.2423 (269)	1.947 (2,161)	9	22	21	**27.0±4.6**	14.27±0.24	1.69 (49)
AK261c	N42.06017/E022.73525	895	Sandstone	A	16	1.329 (4,783)	0.2402 (195)	1.973 (1,601.4)	98	0	19	**30.1±4.6**	15.06±0.10	1.00 (96)
Cenozoic volcaniclastic sediments														
AK72[a]	N42.22276/E022.75477	670	Tuff	Z	16	0.4469 (2,651)	7.526 (1,300)	5.842 (1,009)	21	8	510	**35.1±3.6**		
AK73	N42.22319/E022.75542	652	Tuff	A	18	1.290 (8,505)	0.3222 (332)	1.738 (1,791)	100	0	17	**44.4±5.4**	14.91±0.28	1.11 (16)
				Z	24	0.4401 (2,651)	10.91 (1,979)	7.385 (1,340)	31	8	671	**43.0±3.8**		
AK74	N42.22373/E022.75661	650	Tuff	A	25	1.325 (8,643)	0.5696 (696)	2.890 (3,532)	0	22	27	**50.5±6.4**	12.63±0.75	1.51 (4)
AK76	N42.22664/E022.76065	630	Tuff	A	23	1.412 (4,240)	0.6396 (613)	3.217 (3,083)	15	9	29	**52.3±5.4**	13.29±0.65	1.71 (7)
AK125[a]	N42.23900/E022.46978	940	Pyroclastic	Z	22	0.4156 (2,651)	11.15 (2,235)	8.058 (1,615)	18	7	756	**35.0±3.0**		
AK167[a]	N42.24010/E022.45389	1,150	Tuff	A	20	1.142 (4,310)	0.2498 (287)	1.691 (1,942.7)	94	0	19	**31.1±4.0**	14.87±0.10	0.96 (91)
				Z	7	0.4523 (2,651)	9.644 (456)	8.206 (388)	87	0	708	**32.3±4.6**		
AK199[a]	N42.23859/E022.46449	980	Pyroclastic	A	21	1.085 (4,310)	0.2628 (319)	21.617 (1,963)	59	1	19	**32.7±4.0**	15.14±0.09	0.90 (91)
				Z	20	0.4645 (2,651)	11.21 (3,051)	9.744 (2,652)	0	14	818	**32.9±3.0**		
AK245[a]	N42.22137/E022.81863	595	Pyroclastic	Z	30	0.4357 (2,761)	10.20 (1,948)	7.999 (1527.3)	100	0	716	**33.8±2.6**		
AK302[a]	N42.23859/E022.46449	850	Tuff	A	14	1.413 (4,877)	0.2961 (174)	2.567 (1,508)	99	0	23	**30.3±5.0**	14.74±0.18	0.82 (20)
				Z	36	0.4099 (2,761)	17.17 (3,622)	9.380 (1,979)	0	34	892	**46.9±6.2**		

P(χ^2) is the probability of obtaining χ^2 values for ν degrees of freedom where ν = number of crystals−1

All ages are central ages (Galbraith 1981). $\lambda D = 1.55125 \times 10^{-10}$

A geometry factor of 0.5 was used

Zeta = 372 ± 13 for CN5/apatite, and 132 ± 3 for CN1/zircon

Irradiations were performed at the ANSTO facility, Lucas Heights, Australia

All numbers in brackets are numbers of measurements

ρd, ρs and ρi represent the standard, sample spontaneous and induced track densities, respectively

A apatite, Z zircon, MTL mean track length

[a]Zeta = 372 ± 13 for CN5/apatite, 132 ± 3 which were calculated using a zeta value of 122 ± 2 for CN1/zircon

Fig. 5 Tera-Wasserburg diagrams (Tera and Wasserburg 1972) for sample *AK245* and sample *AK199* (for locations see Fig. 3). *Filled ellipses* on the diagrams to the *right* are those used for age calculations. Data-point error ellipses: 68.3% confidence for all diagrams
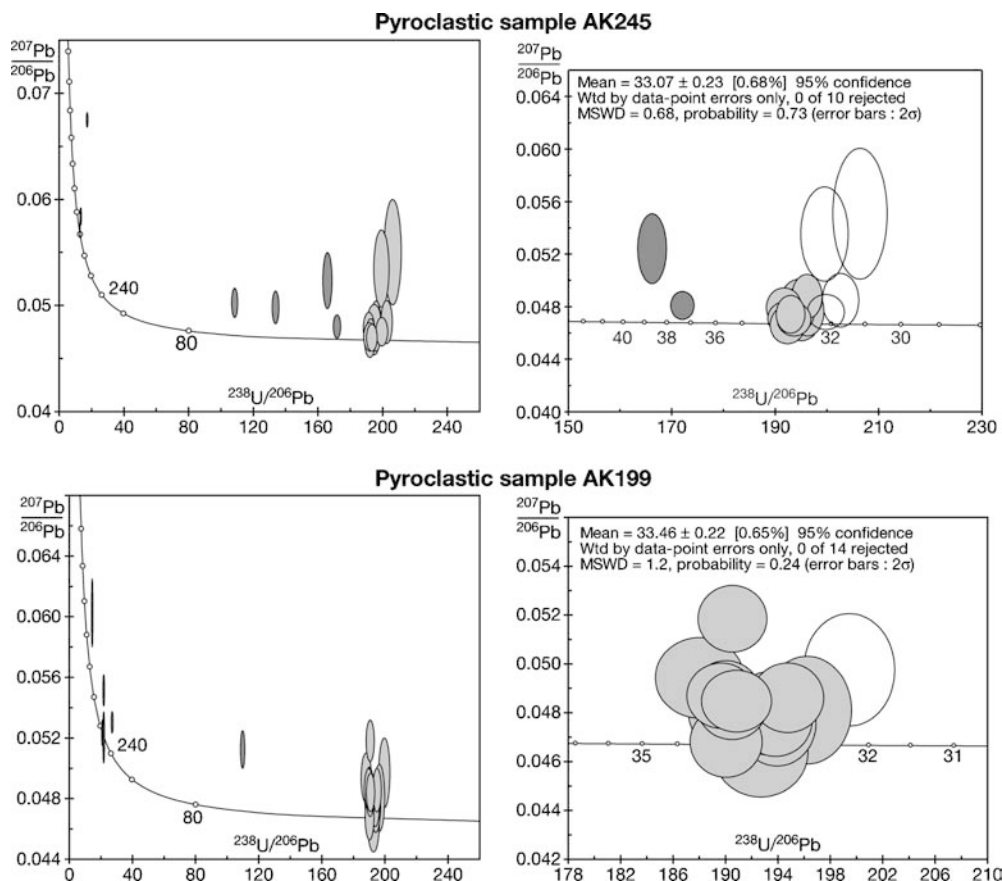

Pyroclastic sample AK245

Pyroclastic sample AK199

Fig. 6 Detrital and volcanic ash population ages vs. stratigraphic position from the Paleogene sediments in the Kraishte area. Different age populations were separated using the method of Sambridge and Compston (1994). *Bold sample numbers* are pyroclastics. Time-scale of Berggren et al. (1995). Formation and member names after Kounov (2003)
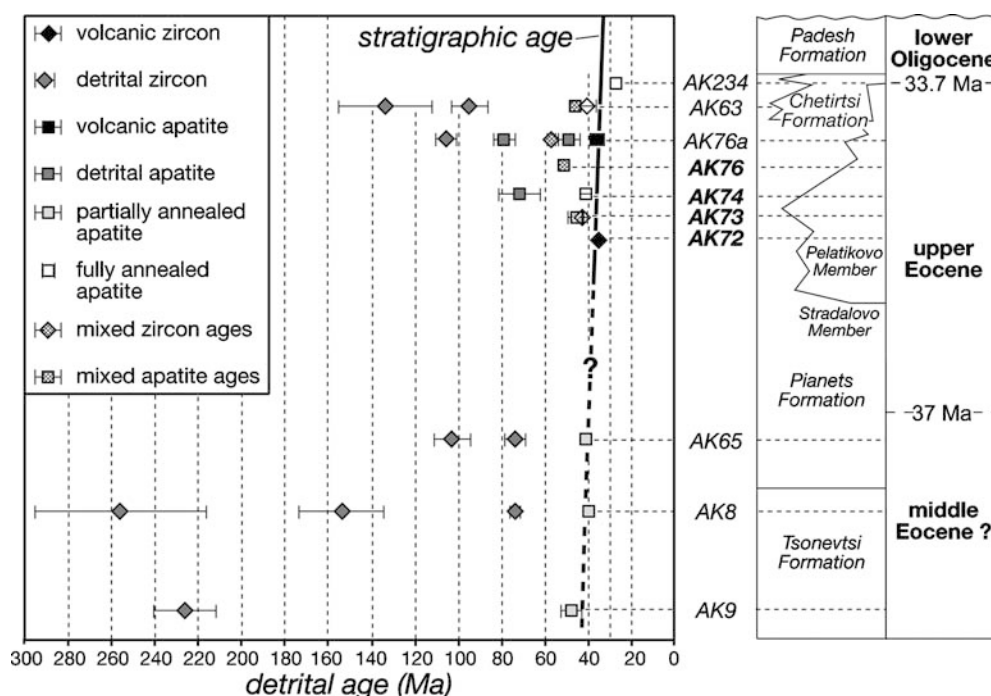
sediments must be older than 35 Ma. A straight line extrapolation to the oldest units extends the age of sedimentation to the latest 40 Ma, (middle Eocene = Bartonian) and puts an upper limit on the initiation of the basins (Zagorchev 2001). This is at least 7 million years after the beginning of extension as determined above.

Fig. 7 *Left column*: modelled thermal histories for the terrigenous sediments of Paleogene basins. The apatite partial annealing zone is within the temperature limits assigned by Laslett et al. (1987). For details of modelling see the Appendix. Boxes constrain the (T–t) space permitted for the modelled paths. *Grey arrows* represent potential paths of cooling before sedimentation. *The shaded vertical area* represents the probable heating event at 45–35 Ma. *Right column*: apatite FT length histograms. *n* number of track lengths measured. *Var* is percent variation from pooled age
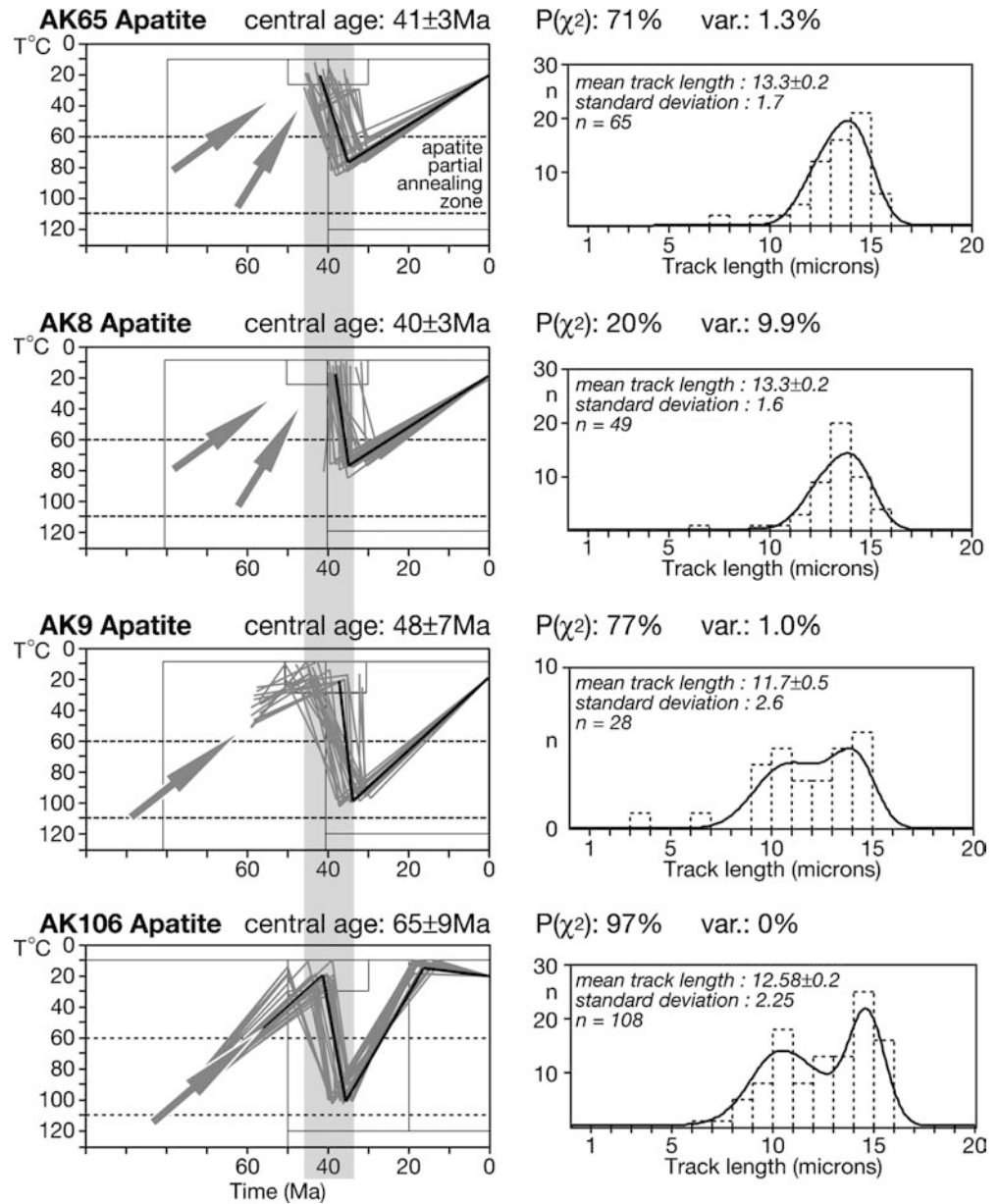
Thermal history Thermal modelling of the apatite FT data from four sedimentary horizons below the ashes (Figs. 3, 6 and 7; samples AK8, AK9, AK65 and AK106) supports the conclusion that the detrital apatites in the lower layers of the basin were partially reset (to between 80 and 100°C) during the time period of 45–35 Ma. This heating event took place almost immediately after sedimentation and lasted until about 35 Ma, when cooling began and lasted until today.

This then implies that the sediments younger than 35 Ma have not been reset. The first line of evidence for lack of resetting in these sediments is the presence of mixed apatite age populations. Secondly, the youngest apatite population in sandstone sample AK76a has an age of 36 Ma (Fig.6). This age is statistically coincident with the volcanic age of the ash AK72 (35 Ma) about 300 m beneath sandstone AK76a. In addition, the

sedimentary overburden, which is estimated to be at most 1,500 m (the thickness of sediments younger than 35 Ma), cannot explain the 80–100°C heating recorded prior to 35 Ma in the bottom sediments.

Sediment source The older detrital zircon ages, dominantly in the lower section but also partly represented higher in the stratigraphic section (Fig. 6) are most likely due to input from the Morava and Struma units, which have older exhumation histories (Table 1).

Sample AK76a has three populations of apatites, 36, 49 and 79 Ma. The first corresponds to the age of the ash immediately below, AK72. The second population is slightly older than the oldest age from the Osogovo–Lisets Complex at the surface today (compare Tables 3 and 4). Thus, it is probable that second population grains are derived from the Osogovo–Lisets Complex.

Table 5 Fission-track analysis

Sample no.	Grid references	Altitude (m)	Lithology	Mineral	No. of grains	ρd (10⁶ cm⁻²)	ρs (10⁶ cm⁻²)	ρi (10⁶ cm⁻²)	P(χ²)(%)	Variation (%)	U conc. (ppm)	Central age (±2σ) Ma	MTL (±1σ) μm	Standard deviation (N) μm
Cenozoic granites sunamb dykes														
AK50	N42.19426/ E022.60363	1,680	Granite	A	20	1.331 (4,618)	0.4997 (424)	3.936 (3,340)	99	0	37	**31.4±3.4**	14.53±0.11	1.04 (89)
				Z	19	0.4943 (2,721)	7.989 (2,896)	8.329 (3,019)	71	0	657	*31.2±2.0*		
AK56	N42.15873/ E022.51826	2,240	Rhyolite	A	22	1.363 (8,505)	0.2023 (203)	1.779 (1,785)	100	0	16	**28.8±4.4**	15.07±0.13	1.01 (60)
				Z	19	0.3952 (2,644)	6.248 (2,159)	5.611 (1,939)	94	0	554	*29.0±2.2*		
AK308	N42.21391/ E022.52854	1,665	Rhyolite	Z	17	0.3797 (2,761)	11.82 (1,973)	9.203 (1,536)	94	0	954	*32.1±2.6*		

$P(\chi^2)$ is the probability of obtaining χ^2 values for ν degrees of freedom where ν = number of crystals−1

All ages are central ages (Galbraith 1981). λD = 1.55125×10⁻¹⁰

A geometry factor of 0.5 was used

Zeta = 372 ± 13 for CN5/apatite, and 132 ± 3 for CN1/zircon

Irradiations were performed at the ANSTO facility, Lucas Heights, Australia

All numbers in brackets are numbers of measurements

ρd, ρs and ρi represent the standard, sample spontaneous and induced track densities, respectively

A apatite, Z zircon, MTL mean track length

These ages represent the time at which the sample was at a temperature of approximately 110°C and was exposed later after further erosion or tectonic denudation, with a lag time of approximately 15 million years. The third population was probably derived from the Morava and Struma units because the age corresponds to the ages obtained from these units at the surface today.

Some sediment samples have single population AFT ages at about 30 Ma (*AK*234, *AK*261*c*, *AK*167, *AK*302); Table 1; Fig. 3). These ages are younger than the estimated stratigraphic age of the enclosing sediments (Kounov 2003) and may again reflect heat advection from igneous activity, which was pervasive at that time (Harkovska and Pecskay 1997).

Comparative cooling

A comparison of the temperature-time path of the footwall with that of the hanging wall (Fig. 10) reveals that heating in the hanging wall, i.e. the Morava and Struma units as well as the sediments, is contemporaneous with the fastest cooling in the footwall. This clearly suggests that heat derived from the rising hot footwall was conducted into the hanging wall as it has been argued in other natural examples (e.g. Van Den Driessche and Brun 1991–1992; Grasemann and Mancktelow 1993; Ehlers et al. 2001).

Thermotectonic evolution

The Osogovo–Lisets Dome has the structural and thermal characteristics of a core complex exhumed during early Cenozoic extension. A retrogressive metamorphic overprint of greenschist-facies (chlorite-ilmenite-clinozoisite) is related to hydrothermal activity during the formation of extensional shear bands, crenulation cleavage, cohesive breccias in which Pb–Zn-ores crystallised (Vardev 1987), and gouges. This overprint mostly affects the cataclastic part of the detachment zone (top of the footwall). The old mineral assemblages show little retrogressive overprint in the deepest structural levels. Probably part of the retrogressive metamorphism (chloritisation and epidotisation) is also associated with the younger magmatic phase, when hydrothermal activity was present.

Fission-track data document rapid cooling in the Osogovo–Lisets Complex in the middle Eocene (Fig. 11a). The younging direction of the FT ages further indicates that the bulk movement along the Eleshnitsa detachment was top-to-the-SW, which is consistent with the relative displacement inferred from slickenside lineations, secondary fractures and shear bands. The Eleshnitsa detachment was the main detachment. The younger Dragovishtitsa detachment was the antithetic fault accommodating the dome formation (Fig. 11b).
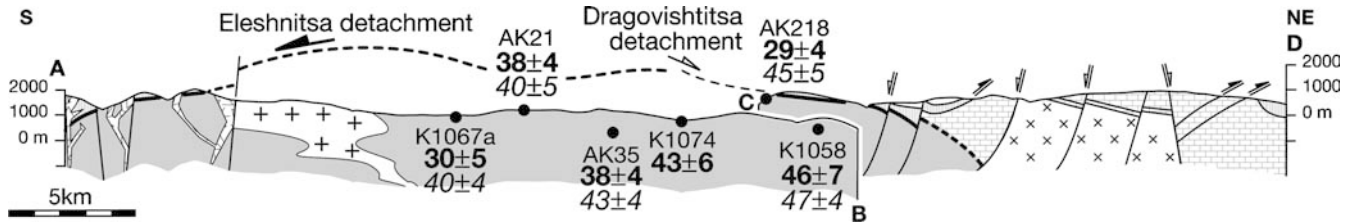
Fig. 8 Sections AB and CD (Fig. 3) with apatite and zircon FT ages. Lithological key as in Fig. 2

In the basins, formation of the alluvial fans was related to faulting along their borders, where large olistoliths were shed from the fault scarps. Formation of the half-graben basins in the hanging wall of the detachments was related to the W–E to SW–NE extension and the resulting NW–SE trending faults controlling sedimentation. By the end of the Eocene, sediments had sealed the inactive detachments. This inactivity may actually correspond to a major change in extension tectonics since it also was the time of marine transgression and volcanic activity (35–32 Ma; Fig. 11c). Furthermore, this also correlates with the termination of the heating phase in the hanging wall.

Extension may have been accompanied by ductile flow and anatexis in the lower crust but these levels were not exhumed in the Osogovo–Lisets core complex (Fig. 11c, d). However, the emplacement of the 32–29 Ma rhyolitic to dacitic subvolcanic bodies and dykes into the Paleogene sediments and their basement, along with intrusion of the Osogovo granite, are strong evidence for melting of the lower crust during the Cenozoic

(Graf 2001). The dykes cut the detachments (Fig. 11d), which also suggests a major change in extension tectonics at about 30 Ma.

Post-Oligocene (Miocene?) brittle deformation (Fig. 11d) was associated with the formation of NW–SE and NNW–SSE sets of normal and strike-slip faults (Bonchev et al. 1960; Moskovski 1969, 1971; Moskovski and Harkovska 1973; Kounov 2003).

Discussion

Our new FT ages indicate that Paleogene extension in the Kraishte lasted between 47 and 30 Ma. This is consistent with the late Eocene sedimentary cover on the detachment and 30 Ma dykes that crosscut the detachment. This extension is much younger than the Late Cretaceous Sredna Gora back arc basin (Aiello et al. 1977) and therefore is not related to the corresponding arc system. On the other hand, such timing is similar to the extension associated with Late Eocene to Late Oligocene magmatism reported in the Balkan and adjacent segments of the Alpine orogenic system (Burchfiel et al. 2000) and orogen-parallel extension in the southern Carpathians (Schmid et al. 1998). It is also contemporaneous with and has a similar trend to the early Cenozoic extension in the
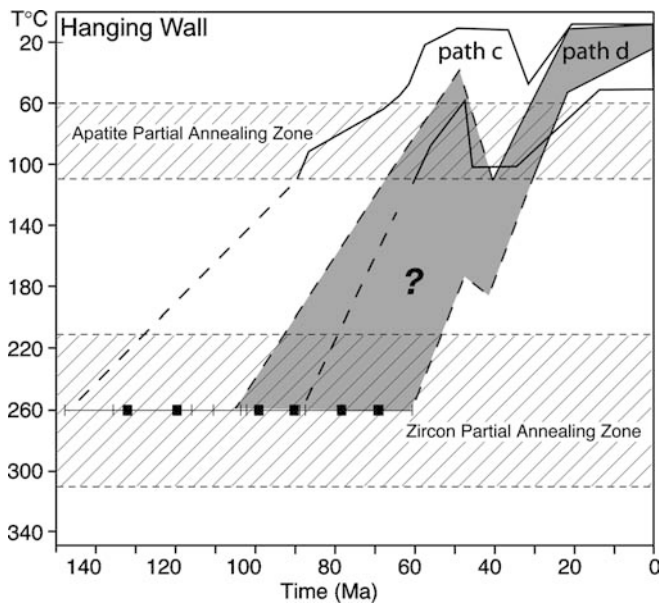

Fig. 9 Modelled T–t paths for the hanging wall samples of the detachment system. *Black squares* represent the zircon FT ages of the modelled samples. *Dashed lines* within the apatite partial annealing zone represent the probable earlier T–t path for the samples from group "d" fully reset during the extension by high heat flow from the footwall or late magmatic activity respectively
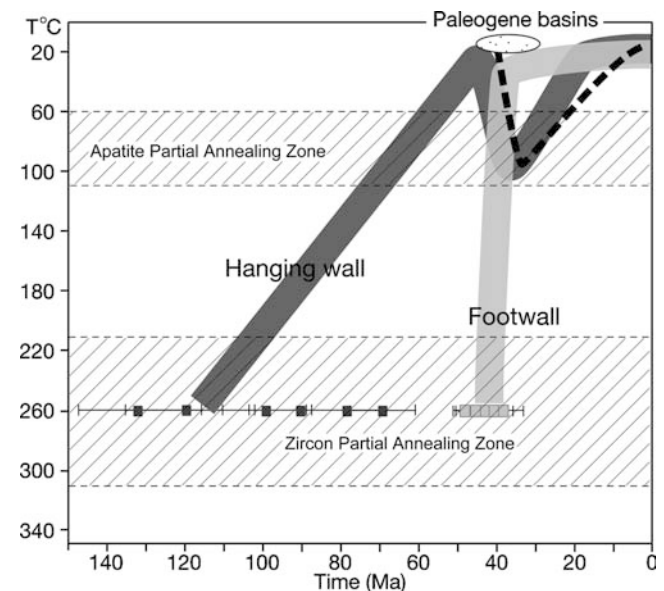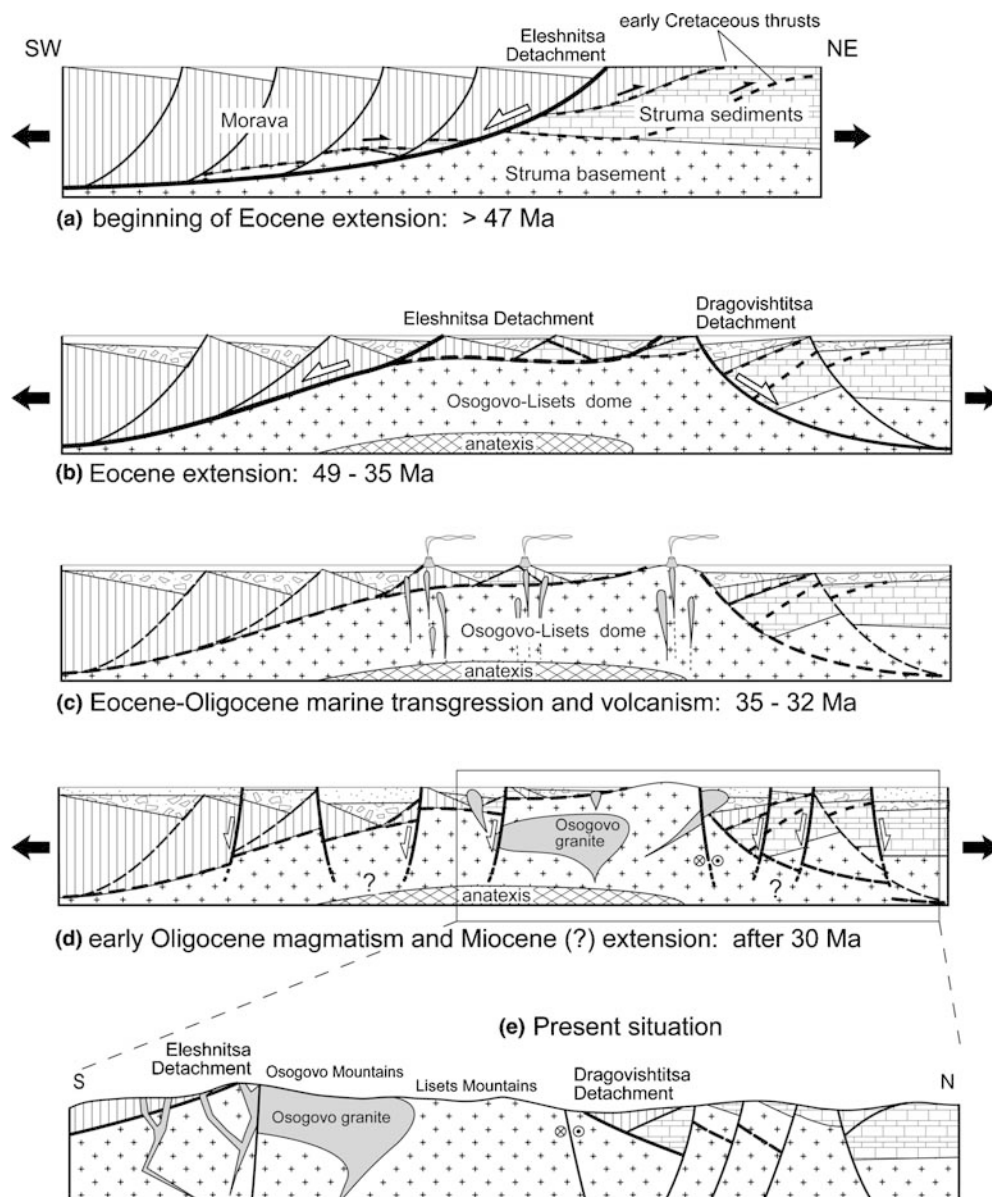

Fig. 10 Modelled T–t paths for the samples from the footwall and hanging wall of the detachment system including those of the sedimentary basins and path "b" of the hanging wall samples (*dashed black line*)

Fig. 11 Proposed evolutionary model of the Kraishte area from middle Eocene to present times

Rhodope (Burg et al. 1996; Ricou et al. 1998). Accordingly, Eocene–Oligocene SW–NE extension was active all around the Carpatho-Balkanic orocline.

It is difficult to decide whether coeval events in the Kraishte and the Rhodope have the same cause. In both cases, early Cenozoic extension fits neither the trend nor the age of the N–S Aegean extension, which dominated the eastern Mediterranean realm since ca. 25 Ma (e.g. Gautier et al. 1999; Burchfiel et al. 2000). It is an older event that might reflect transtension during northeastward drifting, lateral extrusion and rotation of continental fragments around the western boundary of Moesia (Boccaletti et al. 1974; Tapponnier 1977; Burchfiel 1980; Schmid et al. 1998). In the Osogovo–Lisets Complex, the lack of Mesozoic, high-grade mylonitic deformation documented throughout the Rhodope (Burg et al. 1996; Krohe and Mposkos 2002) and the absence of Paleozoic–Mesozoic cover in the Rhodope

lead us to suggest, following Gealey (1988), that the continental fragments around western Moesia, found as slivers in the eastern Carpathians, have a Serbo-Macedonian rather than a Rhodopian affinity.

While extension was taking place in the Kraishte, convergence that dominated the Mediterranean realm led to the closure of the Vardar Ocean and further obduction of its remnants onto the Pelagonian continental fragment (Ricou et al. 1998). Owing to the dominantly rhyolitic and very short-lived magmatism, we do not concur with Burchfiel et al. (2000) that extension took place within a subduction-related arc. Orogen-normal extension of a thickened and thermally weakened continental crust is the most plausible explanation for the formation of the Osogovo–Lisets Complex. This extension event may have been triggered by the shift of the subduction from the Vardar to its current position in the exterior of the Dinaric–Hellenic Belt (Fig. 1).

Conclusions

Examination of the Osogovo–Lisets core complex in the Kraishte, western Bulgaria revealed:

1. Cenozoic extension began before 47 Ma, associated with formation of low-angle detachment faults between the Morava and Struma units in the hanging wall and the Osogovo–Lisets complex in the footwall.
2. Progressive southwestward unroofing and cooling of the Osogovo–Lisets basement along the Eleshnitsa detachment dominated crustal extension and controlled the formation of half-graben sedimentary basins filled initially with continental deposits.
3. During rapid cooling of the hot Osogovo–Lisets footwall, heat was transferred to the hanging wall.
4. Rhyolitic magmatism accompanied syn-extension sedimentation between 35 and 32 Ma.
5. Segments of the detachments were no longer active by the latest Eocene, when sedimentation became marine. Inactivation of the detachment system preceded the emplacement of rhyolitic dykes and magmatic bodies such as the Osogovo granite (31–30 Ma), which caused local heating in the region.
6. Crustal thinning led to the denudation and exhumation of the Precambrian-early Cambrian basement rocks exposed in high-altitude culminations (Osogovo and Lisets Mountains) between low-altitude basins.

We conclude that the Kraishte region underwent a major extensional event in the middle Eocene-early Oligocene. This extension in the southern Balkan is older than, and separated from, the Miocene to Quaternary Aegean extension. Eocene–Oligocene extension was controlled by the distribution of earlier crustal thickening all around the Carpatho-Balkanic orocline, earlier thickening being represented by the Cretaceous emplacement of the Morava Nappe in the Kraishte. The presence of a thickened crust is consistent with the massive rhyolitic volcanism that sealed extension structures in the Kraishte as in the Rhodope. This rhyolitic magmatism reveals voluminous crustal melting in deep root zones and subsequent mass and heat transfer in the crust.

Appendix

Sample preparation followed the routine technique described in Seward (1989). Etching of the apatite grains was done with 7% HNO_3 at 21°C for 50 s. Zircon grains were etched in a eutectic mixture of KOH and NaOH at 220°C for between 4 and 40 h. Irradiation was carried out at the ANSTO facility, Lucas Heights, Australia.

Microscopic analysis was completed using an optical microscope with a computer driven stage (Dumitru 1995). All ages were determined using the zeta approach (Hurford and Green 1983) with a zeta value of 372 ± 13 for CN5 and 132 ± 3 (1998–2000) and 122 ± 2 (2001–2002) for CN1 (see Table 1). They are reported as central ages (Galbraith and Laslett 1993) with a 2σ error (Table 1). The magnification used was 1,250× for apatite and 1,600× (dry) for zircon. Horizontal confined track lengths were measured at 1,250×.

Modelling of the apatite age and track length data was completed with the Monte Trax program of Gallagher (1995), using an initial track length of 15.5 μm (for discussion see Seward et al. 2004). A composition of Durango apatite was used with the Laslett model in this program. Samples were forced to the surface at the time of deposition. Because their previous thermal history is unknown the various pathways are marked by arrows on Fig. 7. We assume an effective closure temperature for apatite of 110 ± 10°C with a partial annealing zone from 110–60°C (Green and Duddy 1989; Corrigan 1993). For zircon, the closure temperature is taken as 260 ± 50°C with a partial annealing zone from 210–310°C (Yamada et al. 1995).

References

Aiello E, Bartolini C, Boccaletti M, Gocev P, Karagjuleva J, Kostadinov V, Manetti P (1977) Sedimentary features of the Srednogorie zone (Bulgaria): an upper Cretaceous intra-arc basin. Sediment Geol 19:39–68

Berggren WA, Kent DV, Swisher CCI, Aubry MP (1995) A revised Cenozoic geochronology and chronostratigraphy. Geochronology, time scales and global stratigraphic correlation. In: Berggren WA, Kent DV, Aubry M-P, Hardenbol J (eds) Geochronology, time scales and global stratigraphic correlation special publication. SEPM (Soc Sediment Geol) Spec. Publ. 54:129–212

Boccaletti M, Manetti P, Peccerillo A (1974) Hypothesis on the plate tectonic evolution of the Carpatho-Balkan Arcs. Earth Planetary Sci Lett 23(2):193–198

Bonchev E (1936) Versuch einer tektonischen Synthese Westbulgariens. Geologica Balcanica 2(3):5–48

Bonchev E, Karagiuleva J, Kostadinov V, Manolov Z, Kamenova J, Dinkov E, Bakalova D, Manolova R (1960) Grundlagen der Tektonik von Kraiste mit den angrenzenden Gebieten. Travaux sur la Géologie de Bulgarie. Série Stratigraphie et Tectonique 1:7–92 (in Bulgarian; abstracts in Russian and German)

Bonev K, Ivanov Z, Ricou L-E (1995) Dénudation tectonique au toit du noyau métamorphique rhodopien-macédonien: la faille normale ductile de Gabrov Dol (Bulgarie). Bulletin de la Société géologique de France 166(1):49–58

Burchfiel BC (1980) Eastern European Alpine System and the Carpathian Orocline as an example of collision tectonics. Tectonophysics 63:31–61

Burchfiel CB, Nakov R, Tzankov T, Royden L (2000) Cenozoic extension in Bulgaria and northern Greece: the northern part of the Aegean extensional regime. In: Bozkurt E, Winchester JA,

Piper JDA (eds) Tectonics and magmatism in Turkey and the surrounding area. Geol Soc Lond Spec Publ 173:325–352

Burg J-P, Ivanov Z, Ricou L-E, Dimor D, Klain L (1990) Implications of shear-sense criteria for the tectonic evolution of the Central Rhodope massif, southern Bulgaria. Geology 18:451–454

Burg J-P, Klain L, Ivanov Z, Ricou L-E, Dimov D (1996) Crustal-scale thrust complex in the Rhodope Massif. Evidence from structures and fabrics. In: Nairn AEM, Ricou L-E, Vrielynck B, Dercourt J (eds) The ocean basins and margins: the Tethys Ocean 8. Plenum Publishing Corporation, New York, pp 125–149

Corrigan JD (1993) Apatite fission-track analysis of Oligocene strata in South Texas, U.S.A.: testing annealing models. Chem Geol 104:227–249

Dewey JF, Pitman III WC, Ryan WBF, Bonin J (1973) Plate tectonics and the evolution of the Alpine System. Geol Soc Am Bull 84:3137–3180

Dimitrov C (1931) Contribution to the geology and petrography of the Konyavo Mountain. Rev Bulgarian Geol Soc 3:3–52 (in Bulgarian)

Dimitrova E (1964) Petrologie des kristallinen Sockels des Osogovo Gebirges. Bull Geol Inst Ser Stratigr Lithol 13:99–110 (in Bulgarian, abstract in German)

Dumitru TA (1995) A new computer automated microscope stage system for fission-track analysis. Nuclear Tracks Radiat Meas 21:575–580

Ehlers TA, Armstrong PA, Chapman DS (2001) Normal fault thermal regimes and the interpretation of low-temperature thermochronometers. Phys Earth Planet Interiors 126:179–194

Galbraith RF, Laslett GM (1993) Statistical models for mixed fission-track ages. Nuclear Tracks Radiat Meas 21:459–470

Gallagher K (1995) Evolving temperature histories from apatite fission-track data. Earth Planet Sci Lett 136:421–435

Gautier P, Brun J-P (1994) Ductile crust exhumation and extensional detachments in the central Aegean (Cyclades and Evvia Islands). Geodinamica Acta 7:57–85

Gautier P, Brun J-P, Moriceau R, Sokoutis D, Martinod J, Jolivet L (1999) Timing, kinematics and cause of Aegean extension: a scenario based on a comparison with simple analogue experiments. Tectonophysics 315:31–72

Gealey WK (1988) Plate tectonic evolution of the Mediterranean—Middle East region. Tectonophysics 155:285–306

Graf J (2001) Alpine tectonics in Western Bulgaria: Cretaceous compression of the Kraishte region and Cenozoic exhumation of the crystalline Osogovo–Lisets Complex. Unpublished PhD Thesis, ETH-Zürich

Grasemann B, Mancktelow NS (1993) Two-dimensional thermal modelling of normal faulting: the Simplon fault zone, Central Alps, Switzerland. Tectonophysics 225:155–165

Green PF, Duddy IR (1989) Some comments on paleotemperature estimation from apatite fission-track analysis. J Petroleum Geol 12:111–114

Harkovska A, Pecskay Z (1997) The Tertiary magmatism in Ruen magmato-tectonic zone (W. Bulgaria)—a comparision of new K–Ar ages and geological data. In: Boev B, Serafimovski T (eds) Magmatism, metamorphism and metallogeny of the Vardar Zone and Serbo-Macedonian Massif. Faculty of Mining Geology, Stip—Dojran, Republic of Macedonia, pp 137–142

Haydoutov I, Kolcheva K, Daieva L (1994) The Struma Diorite Fm from Vlahina block, SW Bulgaria. Rev Bulgarian Geol Soc 55:9–35

Hurford AJ, Green PF (1983) The zeta age calibration of fission-track dating. Isot Geosci 1:285–317

Ivanov Z (1988) Aperçu général sur l'évolution géologique et structurale du massif des Rhodopes dans le cadre des Balkanides. Bulletin de la Société géologique de France (8)4:227–240

Jolivet L, Faccenna C, D'Agostino N, Fournier M, Worrall D (1999) The kinematics of back-arc basins, examples from the Tyrrhenian, Aegean and Japan Seas. In: Mac Niocaill C, Ryan PD (eds) Continental tectonics. Geol Soc Lond Spec Publ 164:21–53

Kilias A, Falakis G, Moundrakis D (1997) Alpine tectonometamorphic history of the Serbomacedonian metamorphic rocks: implications for the Tertiary unroofing of the Serbomacedonian-Rhodope metamorphic complexes (Macedonia, Greece). Miner Wealth 105:9–27

Kober L (1928) Der Bau der Erde. Borntraeger, Berlin, p 499

Kounov A (2003) Thermotectonic evolution of Kraishte, western Bulgaria. Unpublished PhD thesis, ETH-Zürich

Krohe A, Mposkos E (2002) Multiple generation of extensional detachments in the Rhodope Mountains (northern Greece) evidence of episodic exhumation of high-pressure rocks. In: Blundell DJ, Neubauer F, von Quadt A (eds) The timing and of major ore deposits in an evolving orogen. Geol Soc Lond Spec Publ 204:151–178

Laslett GM, Green PF, Duddy IR, Gleadow AJW (1987) Thermal annealing of fission tracks in apatite; 2. A quantitative analysis. Chem Geol 65:1–13

Liati A, Gebauer D (1999) Constraining the prograde and retrograde P-T-t path of Eocene H P rocks by SHRIMP dating of different zircon domains: inferred rates of heating, burial, cooling and exhumation for central Rhodope, northern Greece. Contrib Miner Petrol 135:340–354

Lister GS, Banga G, Feenstra A (1984) Metamorphic core complexes of Cordilleran type in the Cyclades, Aegean Sea, Greece. Geology 12(4):221–225

Moskovski S (1968) Tectonic of the Pianec grabens complex south of Kjustendil. Bull Geol Inst Ser Stratigr Lithol 17:143–158 (in Russian)

Moskovski S (1969) Tektonik eines Teiles des Pijanec-Grabenkomplexes südlich von Kjustendil. Störungen. Annuaire de l'Université de Sofia, Faculté de Géologie et Géographie 1(61):141–156 (in Bulgarian, abstract in German)

Moskovski S (1971) On the sequence in the formation of Paleogene–Neogene graben structures in the Kraishtides in Bulgaria. Rev Bulgarian Geol Soc 32(1):21–31 (In Bulgarian, abstract in English)

Moskovski S, Harkovska A (1973) Main stages in the Late Alpine development of some fault zones in a part of South-Western Bulgaria. Annuaire de l'Université de Sofia, Faculté de Géologie et Géographie 1(65):73–84 (in Bulgarian, abstract in English)

Moskovski S, Shopov V (1965) Stratigraphy of the Paleogene and the resedimentation phenomena (olistostromes) related to it in Pyanets area, Kjustendil district (SW Bulgaria). Bull Geol Inst Sofia Stratigr Lithol 16:189–209 (In Bulgarian, abstract in English)

Petrov N (2001) Petrostructural studies in the southern and southeastern parts of the Osogovo–Lisets dome. Unpublished Diploma thesis, Sofia

Ricou L-E (1994) Tethys reconstructed: plates, continental fragments and their boundaries since 260 Ma from Central America to South-eastern Asia. Geodinamica Acta 7:169–218

Ricou L-E, Burg J-P, Godfriaux I, Ivanov Z (1998) Rhodope and Vardar: the metamorphic and the olistostromic paired belts related to the Cretaceous subduction under Europe. Geodinamica Acta 11:285–309

Schmid SM, Berza T, Diaconescu V, Froitzheim N, Fügenschuh B (1998) Orogen-parallel extension in the southern Carpathians. Tectonophysics 297:209–228

Seward D (1989) Cenozoic basin histories determined by fission-track dating of basement granites, South Island, New Zealand. Chem Geol (Isotope Geoscience Section) 79:31–48

Seward D, Grujic D, Schreurs G (2004) An insight into the breakup of Gondwana—identifying events through low temperature thermochronology from the basement rocks of Madagascar. Tectonics 23:TC3007, doi:10.1029/2003TC001556

Spassov C (1973) Stratigraphie des Devons in Sudwest-Bulgarien. Bull Geol Inst Ser Stratigr Lithol 22:5–38 (in Bulgarian, abstract in German)

Stampfli G, Marcoux J, Baud A (1991) Tethyan margins in space and time. Palaeogeogr Palaeoclimatol Palaeoecol 87:373–409

Stephanov A, Dimitrov Z (1936) Geologische Untersuchungen im Kustendiler Gebiet. Rev Bulgarian Geol Soc 8(3):1–28 (in Bulgarian, abstract in German)

Tapponnier P (1977) Evolution tectonique du système alpin en Méditerranée: poinçonnement et écrasement rigide-plastique. Bulletin de la Société géologique de France 7–19:437–460

Tera F, Wasserburg GJ (1972) U–Th–Pb systematics in three Apollo 14 basalts and problem of initial Pb in lunar rocks. Earth Planet Sci Lett 14:281–304

Van Den Driessche J, Brun J-P (1991–1992) Tectonic evolution of the Montagne Noire (French Massif Central): a model of extensional gneiss dome. Geodinamica Acta 5:85–99

Vardev N (1987) Structure of the Ruen ore district. Unpublished PhD Thesis, Sofia

Yamada R, Tagami T, Nishimura S, Ito H (1995) Annealing kinetics of fission tracks in zircon: an experimental study. Chem Geol 122:249–258

Zagorchev I (1980) Early Alpine deformations in the red beds within the Poletinci-Skrino fault zone. I. Lithostratigraphic features in light of structural studies. Geologica Balcanica 10(2):37–60 (in Russian, abstract in English)

Zagorchev I (1984) The importance of overthrusts in the Alpine structure of Kraistids. Geologica Balcanica 14(4):37–64 (in Russian, abstract in English)

Zagorchev I (1993) Radomir and Bosilegrad map sheets: explanatory notes. In: Geological map of Bulgaria on scale 1:100 000, Sofia

Zagorchev IS (1996) Geological heritage of the Balkan Peninsula: geological setting (an overview). Geologica Balcanica 26(2): 3–10

Zagorchev I (2001) Introduction to the geology of SW Bulgaria. Geologica Balcanica 31(1–2):3–52

Zagorchev I, Ruseva M (1982) Nappe structure of the southern parts of the Osogovo Mts. and the Pijanec region (SW Bulgaria). Geologica Balcanica 12(3):35–57 (in Russian, abstract in English)

Zagorchev I, Ruseva M (1993) Kriva Palanka and Kjustendil map sheets: explanatory notes. In: Geological map of Bulgaria on scale 1:100 000, Sofia

Zagorchev I, Popov P, Ruseva M (1989) Paleogene stratigraphy in a part of SW Bulgaria. Geologica Balcanica 19(6):41–69 (In Russian, with English abstract)